Characterization of the SECIS binding protein 2 complex required for the co-translational insertion of selenocysteine in mammals

Scott A. Kinzy, Kelvin Caban and Paul R. Copeland*

Department of Molecular Genetics, Microbiology and Immunology, UMDNJ—Robert Wood Johnson Medical School, Piscataway, NJ 08854, USA

ABSTRACT

Selenocysteine is incorporated into at least 25 human proteins by a complex mechanism that is a unique modification of canonical translation elongation. Selenocysteine incorporation requires the concerted action of a kink-turn structural RNA (SECIS) element in the 3′ untranslated region of each selenoprotein mRNA, a selenocysteine-specific translation elongation factor (eEFSec) and a SECIS binding protein (SBP2). Here, we analyze the molecular context in which SBP2 functions. Contrary to previous findings, a combination of gel filtration chromatography and co-purification studies demonstrates that SBP2 does not self-associate. However, SBP2 is found to be quantitatively associated with ribosomes. Interestingly, a wild-type but not mutant SECIS element is able to effectively compete with the SBP2 ribosome interaction, indicating that SBP2 cannot simultaneously interact with the ribosome and the SECIS element. This data also supports the hypothesis that SBP2 interacts with one or more kink turns on 28S rRNA. Based on these results, we propose a revised model for selenocysteine incorporation where SBP2 remains ribosome bound except during selenocysteine delivery to the ribosomal A-site.

INTRODUCTION

Selenocysteine (Sec), the twenty-first amino acid, is incorporated into at least 25 human proteins at specific UGA codons that are decoded by the Sec-tRNA[Ser]Sec (1,2). This tRNA is not sufficient for nonsense suppression because at least two protein factors and one additional *cis*-sequence are required for Sec incorporation. The *cis*-sequence is termed a Sec insertion sequence (SECIS) element that is found in all eukaryotic selenoprotein mRNA 3′ untranslated regions, and was originally thought to be the sole RNA element required for Sec incorporation. This concept has been recently challenged, however, by the discovery of a stem–loop sequence in the coding region of selenoprotein N that is able to support UGA readthrough in the absence of a SECIS element, albeit for both UGA and UAG codons (3). Mammalian Sec incorporation also requires the function of a Sec-specific translation elongation factor (eEFSec/mSelB) that specifically and exclusively binds to the Sec-tRNA[Ser]Sec (4,5). In addition, two specific binding partners have been identified for the SECIS element: SECIS binding protein 2 (SBP2) and ribosomal protein L30 (rpL30). SBP2 is required for Sec incorporation (6), while L30 has thus far been shown to enhance Sec incorporation in transfected cells (7).

SBP2 from the rat (*Rattus norvegicus*) is a 94 kDa protein with orthologues found in species ranging from *Plasmodium falciparum* to mammals. Structure–function analysis of SBP2 has shown that it is comprised of three distinct domains: an N-terminal domain for which a function has not yet been identified, a central 'functional domain' that is required for Sec incorporation but not SECIS element binding, and a C-terminal SECIS element binding domain (8). The latter two domains comprising the C-terminal 447 amino acids are sufficient for all three known biological activities of SBP2: Sec incorporation, SECIS element binding and ribosome binding (8,9). The SBP2 SECIS element binding domain has at its core an L7Ae RNA binding motif that is known to be required for interacting with RNA elements known as kink turns for several ribosomal proteins including rpL30 (10,11), although this core motif is not sufficient for SECIS element binding (8). The L7Ae RNA binding motif is used by rpL30 for both mRNA and 28S rRNA interactions (12), thus providing the best explanation for the competition between SBP2 and L30 for SECIS element binding (7). SBP2 also binds to ribosomes and 28S rRNA (8), and it has been proposed that SBP2 makes ribosome contacts at one or more kink-turn

motifs, but the specific ribosome binding site has not been identified. Several reports have also suggested that SBP2 may exist as a homomultimer based on glycerol gradient sedimentation and the appearance of higher molecular weight complexes during electrophoretic mobility shift assays (7,8,13,14). These results led to a model where SBP2 could simultaneously interact with the ribosome and a SECIS element by having two RNA binding motifs available, one for SECIS element binding and the other for 28S kink-turn binding (15).

In this report, we characterized the aggregate molecular weight of both full-length (FLSBP2) and C-terminal SBP2 (CTSBP2) with a variety of N-terminal tags. These studies were carried out in the context of pull-down and ribosome binding experiments, which compel us to significantly alter our model for Sec incorporation such that SBP2 cannot simultaneously interact with the ribosome and the SECIS element.

MATERIALS AND METHODS

Expression and purification of recombinant proteins

The nucleotide sequence corresponding to full-length rat SBP2 as well as the fully functional C-terminal half of SBP2 (amino acids 399–846) were amplified by PCR and subcloned into pTrcHis by TOPO-TA cloning according to the manufacturer's protocol (Invitrogen) to generate Xpress/His (XH) tagged constructs (XH-FLSBP2 and XH-CTSBP2), which were subsequently transformed into *E.coli* strain BL21 (Promega). The transformed bacteria were grown in LB medium to a density of $\sim$1.0 OD_{600}, and then induced with isopropyl-β-D-thiogalactoside (0.24 mg/ml; Fisher Biotech) for 1.5 h at 30°C. The cells were pelleted, resuspended in Buffer XH (50 mM Sodium Phosphate, pH 8.0, 1 M NaCl, 1% Tween-20, 50 mM imidazole) with protease inhibitors (Complete, Roche) and lysed by freeze–thaw followed by sonication for 10 s/ml. The sonicate was then centrifuged at 15 000 *g* for 15 min at 4°C. The supernatant was applied directly to a 1 ml HiTrap Chelating HP affinity column (GE Healthcare) charged with 10 mg/ml nickel sulfate hexahydrate (Sigma), and tagged protein was eluted in Buffer XH with a linear 50–500 mM imidazole gradient. Strep-tagged CTSBP2 (ST-CTSBP2) was purified as previously described (9).

Untagged CTSBP2 was created by deleting the Xpress/His tags from the XH-CTSBP2/pTrcHis construct by mutagenic PCR. A primer that loops out the Xpress/His tag sequence was used to amplify the entire pTrcHis plasmid using Pfu Turbo (Stratagene). After inducing protein expression as for XH-CTSBP2, the cells were pelleted, resuspended in phosphate-buffered saline (PBS) containing protease inhibitors (Complete, Roche) and 2 mM DTT and lysed by freeze–thaw followed by sonication for 10 s/ml. The sonicate was then centrifuged at 15 000 *g* for 15 min at 4°C. Expression was verified via western blot (see below) and total protein concentration was determined by the Bradford (Bio-Rad) assay.

GST-tagged CTSBP2 (GST-CTSBP2) was created using the same method as described for XH-CTSBP2 except the PCR product was TOPO-TA cloned into pDEST15 (Invitrogen) bearing an in-frame N-terminal GST tag. The resulting plasmid was transformed into *E.coli* strain BL21 (Promega).

For the co-expression of GST-CTSBP2 and XH-CTSBP2, we created XH-CTSBP2 in pCRII-TOPO (Invitrogen) by amplifying XH-CTSBP2 out of pTrcHis including the Trc promoter region. This fragment was TOPO-TA cloned into pCRII-TOPO, which lacks a bacterial promoter and contains both ampicillin (Amp) and kanamycin (Kan) resistance genes. The ampicillin resistance gene was deleted by digesting the plasmid with Xmn I and Ahd I, polishing overhangs with T4 DNA polymerase (Invitrogen) and re-ligating the plasmid with blunt-end ligation using T4 DNA ligase as per the manufacturer's protocol (Invitrogen). Ligated plasmids were transformed into DH5α by electroporation. Kan-resistant colonies were screened for the loss of Amp resistance by streaking individual colonies on Amp-containing plates. Plasmid DNA was isolated from Kan-resistant/Amp-sensitive colonies, and transformed into BL21. The cells were grown in LB medium containing 100 μg/ml Amp and 50 μg/ml Kan to a density of $\sim$1.0 OD_{600} and then induced with L-(+)-arabinose (0.2%; Sigma) and isopropyl-β-D-thiogalactoside (0.24 mg/ml; Fisher Biotech) for 1.5 h at 30°C. The cells were pelleted, resuspended in PBS with protease inhibitors and lysed by freeze–thaw followed by sonication for 10 s/ml. The sonicate was then centrifuged at 15 000 *g* for 15 min at 4°C. The supernatant was applied directly to a 1 ml GSTrap FF affinity column (GE Healthcare) equilibrated in PBS, pH 7.3 and tagged protein was eluted in 50 mM Tris–HCl, pH 8.0 containing 10 mM reduced glutathione (Sigma): 20 μl of each fraction was resolved by 12% SDS–PAGE, transferred to nitrocellulose and probed with a 1:10 000 dilution of anti Xpress-tag antibody (Invitrogen).

Gel filtration chromatography

Two gel filtration chromatography columns were run using a Beckman System Gold HPLC system (126 pumps and 168 diode array detector). A 10 × 300 mm Superdex 200 HR 10/30 (GE Healthcare) column was run at 0.4 ml/min to analyze proteins in the 10–600 kDa range to yield 0.4 ml fractions. A 10 × 500 mm column containing Sephacryl S-500 High Resolution resin (GE Healthcare) was run at 0.5 ml/min to analyze proteins in the 40–2000 kDa range to yield 0.5 ml fractions. Prior to the injection of sample, the columns were equilibrated with a minimum of 2 column volumes of PBS plus 2 mM DTT (PBSD). Purified recombinant SBP2 proteins were exchanged to PBSD by desalting on a 16 × 100 mm column at 2 ml/min. For all molecular weight determinations, 75 μg of purified protein was used. SBP2 content in each fraction was determined either by SDS–PAGE or Sec incorporation activity using luciferase constructs as previously described (9). Sizing of SBP2 was performed by comparison with standards run under conditions identical to those for each type of SBP2 chromatography: thyroglobulin (669 kDa), apoferritin (443 kDa), β-Amylase (200 kDa), alcohol dehydrogenase (150 kDa), bovine serum albumin (66 kDa), carbonic anhydrase (29 kDa) and cytochrome C (12.4 kDa).

For the mixtures of SBP2 and rat testis extract, 0.4 μg of recombinant purified SBP2 was mixed with 15 mg rat testis extract made ribosome-free by centrifugation at 300 000 *g* for 1 h in a Sorvall S80-AT3. Depletion of ribosomes was confirmed by isolating total RNA from a portion of the extract prior to and after centrifugation and resolving the RNA on a

1% agarose gel to confirm the loss of detectable rRNA by ethidium bromide staining.

For the resolution of native SBP2 complexes, a rat hepatoma cell line (McArdle 7777) stably expressing V5/His-tagged FLSBP2 (HV-FLSBP2) (see below) was grown to ~80% confluence in 78 cm^2 plates, cells were rinsed with PBS then lysed in PBSD by scraping followed by dounce homogenization (10 strokes with a high clearance pestle). Crude extracts were centrifuged for 15 min at 14 000 *g* in an Eppendorf 5810 R centrifuge. The supernatant was removed and 500 μl aliquots were injected onto the Sephacryl S-500 column. Protein from each fraction was precipitated by adding trichloroacetic acid and Tween-20 to a final concentration of 8% and 0.1%, respectively. Protein pellets were recovered by centrifugation and washed in 60 μl 100% ethanol then resuspended in 40 μl SDS–PAGE sample buffer of which 20 μl was analyzed by SDS–PAGE, transferred to nitrocellulose and probed with a 1:10 000 dilution of anti-V5 antibody (Invitrogen).

Stable cell lines

V5/His-tagged FLSBP2 was subcloned into the tetracycline-inducible plasmid, pCDNA4-TO-E (Invitrogen) by recombination from a pUni/V5-His-TOPO plasmid containing a FLSBP2 insert. The resulting plasmid was transfected into McArdle 7777 cells stably expressing the tetracycline repressor from pCDNA6/TR using Lipofectamine (Invitrogen). Clones were selected in 500 μg/ml Zeocin and 2 μg/ml blasticidin. Pools of clones were grown to 80% confluence and analyzed as described above.

Sec incorporation assays

Recombinant SBP2 was added to a rabbit reticulocyte lysate (Promega) Sec incorporation assay as indicated in the figure legends. Total reaction volume was 6 μl, which included 25 ng of luciferase reporter construct bearing a Sec (UGA) codon at position 258 as described (9). The reactions were incubated for 1 h at 30°C then diluted with 50 μl of PBS. Luminescence was detected in a Dynex MLX plate luminometer using 50 μl luciferase assay substrate (Promega).

Densitometry

Densitometry was used for three quantitative measures: (i) To quantify relative SBP2 levels on Coomassie-stained gels containing gel filtration fractions. (ii) To quantify absolute SBP2 amounts based on an ovalbumin standard. (iii) To quantify signals from western blot analysis captured on X-ray film. Bands of interest were quantified using ImageJ software (Wayne Rasband, National Institutes of Health).

Western blot analysis

Western blot analysis was performed on fractions containing lower levels of SBP2 as indicated in the figure legends. SDS–PAGE gels were blotted to nitrocellulose membrane (GE Healthcare), rinsed in Tris-buffered saline plus 0.1% Tween-20 (TBST), blocked for 1 h in TBST plus 5% non-fat dried milk then probed using the primary antibodies indicated overnight at 4°C. Antigens were visualized using the SuperSignal West Femto kit (Pierce) according to the manufacturer's protocol.

Affinity-purified anti-SBP2 antibody was made by resolving 5 μg XH-CTSBP2 by SDS–PAGE followed by transfer to nitrocellulose. The protein containing band was detected by Ponceau S staining and excised. The excised strip was incubated with 10 μl of crude polyclonal anti-CTSBP2 antisera in 1 ml of blocking solution. After rotation at 4°C overnight, the strip was subjected to three 15 min washes in TBST. The bound antibody was eluted in 150 μl of 0.1 M Glycine pH 2.5 for 1 min. The eluent was removed from the strip, and 15 μl of 1 M Tris–HCl pH 8.0 was then added to neutralize the mixture. This preparation was diluted into 10 ml blocking solution and used without any further dilution to probe immunoblots as indicated.

Ribosome binding assays

Fifty microliter reaction in PBSD contained 6.0 pmol of XH-CTSBP2 in the presence or absence a 5-fold molar excess of wild-type or mutant radiolabeled GPX4 SECIS RNA for 10 min at 37°C. Next, a 2.5-fold excess (with respect to XH-CTSBP2) of salt-washed ribosomes purified from McArdle 7777 cells as described below was added and incubated for an additional 5 min at 37°C. SBP2 only reactions were supplemented with 2 mg/ml bovine serum albumin as carrier: 45 μl of the mixture was layered onto a 200 μl of 20% sucrose cushion in PBSD and spun at 300 000 *g* for 30 min at 4°C in a Sorvall S80-AT2 rotor. The supernatant was removed and the pellet was re-suspended in 50 μl of 0.5% SDS: 5% of each (supernatant and pellet) was resolved by 12% SDS–PAGE, blotted to nitrocellulose and probed with 1:10 000 dilution of crude anti-SBP2 polyclonal antibody.

For the competition studies during *in vitro* translation, untagged FLSBP2 was translated in the presence of ^{35}S-Met for 30 min in a 200 μl rabbit reticulocyte reaction (Promega). Aliquots of 25 μl were prepared and equal volumes of either water or *in vitro* transcribed GPX-4 mRNA was added and allowed to translate for another 30 min. Subsequently, EDTA was added to the reactions to a final concentration of 5 mM, and tubes were mixed and briefly centrifuged: 20 μl of each reaction was layered over a 200 μl 20% sucrose cushion. Samples were spun as described for the *in vitro* assay: 5% of supernatants and pellets were run on a 12% SDS–PAGE gel, which were fixed and dried. Radiolabeled SBP2 was detected by PhosphorImaging, and bands were quantified using ImageQuant software (GE Healthcare).

Radiolabeling SECIS RNAs

Wild-type and mutant rat GPX4 SECIS element RNAs were transcribed from Hind III linearized plasmids bearing a 217 nt insert derived from the GPX4 3' untranslated region (16). RNA was transcribed with T7 RNA polymerase (Promega) according to the manufacturer's protocol except that 1 μl of [α-^{32}P]UTP was added. RNAs were purified by diluting the reactions to 50 μl with water and extracting with an equal volume of 1:1 phenol:chloroform followed by buffer exchange in a Micro Bio-Spin chromatography column (Bio-Rad). To isolate radiolabeled SECIS RNA from the supernatant and pellet fractions, 1 ml of Trizol (Invitrogen) was added, and RNA was extracted as per the manufacturer's protocol. RNA pellets were re-suspended in 20 μl of nuclease-free water,

and 5 μl was resolved in a 5% denaturing gel (6 M urea, 1× TAE) followed by PhosphorImager analysis.

Ribosome purification

Ribosomes were purified from McArdle 7777 cells grown to 80–100% confluence as adapted from a previously described preparation of yeast 80S salt-washed ribosomes (17). Briefly, cells from ten 78 cm² plates were scraped and collected in 1 ml ribosome buffer per plate (100 mM KOAc, 20 mM HEPES–KOH, pH 7.6, 2.5 mM Mg(OAc)$_2$, 2 mM DTT, 1 mg/ml of heparin and 1× Complete protease inhibitors (Roche). Cells were lysed by dounce homogenizing with a high clearance pestle for 10 strokes on ice and extracts were spun at 17 000 *g* for 15 min (all spins were performed at 4°C in a Sorvall S80-AT3 rotor). To pellet ribosomes, the supernatant was spun at 300 000 *g* for 45 min. After rinsing the ribosomal pellets in 0.5 ml of ribosome buffer, the pellets were resuspended in 2.5 ml of high-salt buffer (ribosome buffer plus 500 mM KCl) and stirred for 30–90 min. To clear insoluble material, samples were spun at 14 000 *g* for 10 min and the supernatant was transferred to a new tube. This step was performed several times until no visible pellet could be seen. Finally, cleared ribosomes were transferred on top of a 0.5 ml of 1 M sucrose cushion in high-salt buffer and spun at 300 000 *g* for 30 min. Ribosomal pellets were re-suspended in 0.1 ml of PBSD and stored in aliquots at −80°C.

RESULTS

Gel filtration chromatography of recombinant SBP2

Previous work has suggested that the fully functional C-terminal half of SBP2 bearing an N-terminal Strep-tag (ST-CTSBP2) exists in a self-associated complex (8). In order to define the aggregate molecular weight of purified ST-CTSBP2, we performed Sephadex 200 gel filtration chromatography. As shown in Figure 1A, ST-CTSBP2 (which has a predicted molecular weight of 51 kDa) elutes both in the void fraction (>1300 kDa) as well as into the included fraction but outside the upper limit of separation range (600 kDa), suggesting a distribution of high molecular weight complexes. To assess the contribution of the Strep-tag, if any, to the aggregate molecular weight, both C-terminal and full-length SBP2 bearing N-terminal Xpress/His tags (XH-CTSBP2 and XH-FLSBP2, respectively) were purified from *E.coli* extracts. These proteins, when chromatographed under conditions identical to those for ST-CTSBP2, eluted as single peaks corresponding to 195 and 390 kDa, respectively (Figure 1A). The expected molecular weights for these proteins are 54 and 97 kDa, respectively, suggesting that self-association may account for the difference between observed and expected molecular weight. To examine the stability of the apparent homomultimeric complexes formed, each of the proteins described above were subjected to gel filtration chromatography in the presence of 1 M NaCl to disrupt electrostatic interactions. As shown in Figure 1A, high-salt conditions disrupted the Strep-tag dependent complex but not the XH-tagged complexes. In fact, the high ionic strength conditions seem to have caused conformational changes or aggregation that yielded higher calculated molecular weights than in

low salt (265 kDa for XH-CTSBP2 and 550 kDa for XH-FLSBP2). These results allow us to conclude that the Strep-tag causes SBP2 to aggregate into large salt-sensitive complexes, consistent with previous indications of complex formation in glycerol gradient sedimentation experiments (8). In addition, it appears that XH-tagged SBP2 forms a salt-stable complex at a discrete size that would predict tetrameric SBP2.

Since Strep-tagged and XH-tagged SBP2 display markedly different properties during gel filtration, we tested Sec incorporation activity for each form of the protein. For this determination, a limiting amount (10 ng) of purified ST-CTSBP2, XH-CTSBP2 or XH-FLSBP2 was tested for Sec incorporation activity as described above. Figure 1B shows that this amount of SBP2, which is in the linear range of activity response (data not shown), resulted in over a 100-fold increase in Sec incorporation as measured by luciferase activity. This response is dependent on both the UGA codon and a wild-type SECIS element (data not shown). Figure 1C shows these data re-plotted as a function of SBP2 concentration in order to directly compare specific activities. Surprisingly, although all of the ST-CTSBP2 is found to be aggregated into large molecular weight complexes (Figure 1A), it is only ~2-fold less active than either XH-CTSBP2 or XH-FLSBP2. These results also confirm the fact that there is no significant difference between *in vitro* Sec incorporation activity of full-length and C-terminal SBP2 (9).

SBP2 homomeric complexes are not observed in pull-down experiments

We tested the ability of SBP2 to interact with itself by co-expressing CTSBP2 with an N-terminal GST tag (GST-CTSBP2) and XH-CTSBP2 in *E.coli* and determined whether XH-CTSBP2 would co-purify with GST-CTSBP2 on glutathione agarose. Fractions obtained from the glutathione column were analyzed by SDS–PAGE on which GST-CTSBP2 but not XH-CTSBP2 was detectable after Coomassie staining (Figure 2A). To verify the lack of XH-CTSBP2 in GST-CTSBP2 containing fractions, a western blot of the same gel was probed with affinity-purified anti-SBP2 antibody. Figure 2B shows that XH-CTSBP2 was not recovered on glutathione agarose indicating that SBP2 does not self-associate even under conditions where co-translational association is possible. The converse purification was performed where XH-CTSBP2 was purified on a nickel agarose column from which GST-CTSBP2 was not co-purified (data not shown). These results are consistent with traditional pull-down experiments using a variety of tags and matrices, none of which showed any evidence of SBP2 self-association (data not shown).

Gel filtration of untagged CTSBP2

Since the pull-down experiments clearly indicate that SBP2 is monomeric, we tested the role of the XH tag in altering the retention times for SBP2 by subjecting untagged SBP2 in crude *E.coli* extract to the same procedure. We found that it elutes near the void volume in low salt but at 190 kDa in high salt (Figure 3). Since the only conserved feature between mammalian Sec incorporation and that in *E.coli* is the ribosome, and considering the size of the complex, we assume that
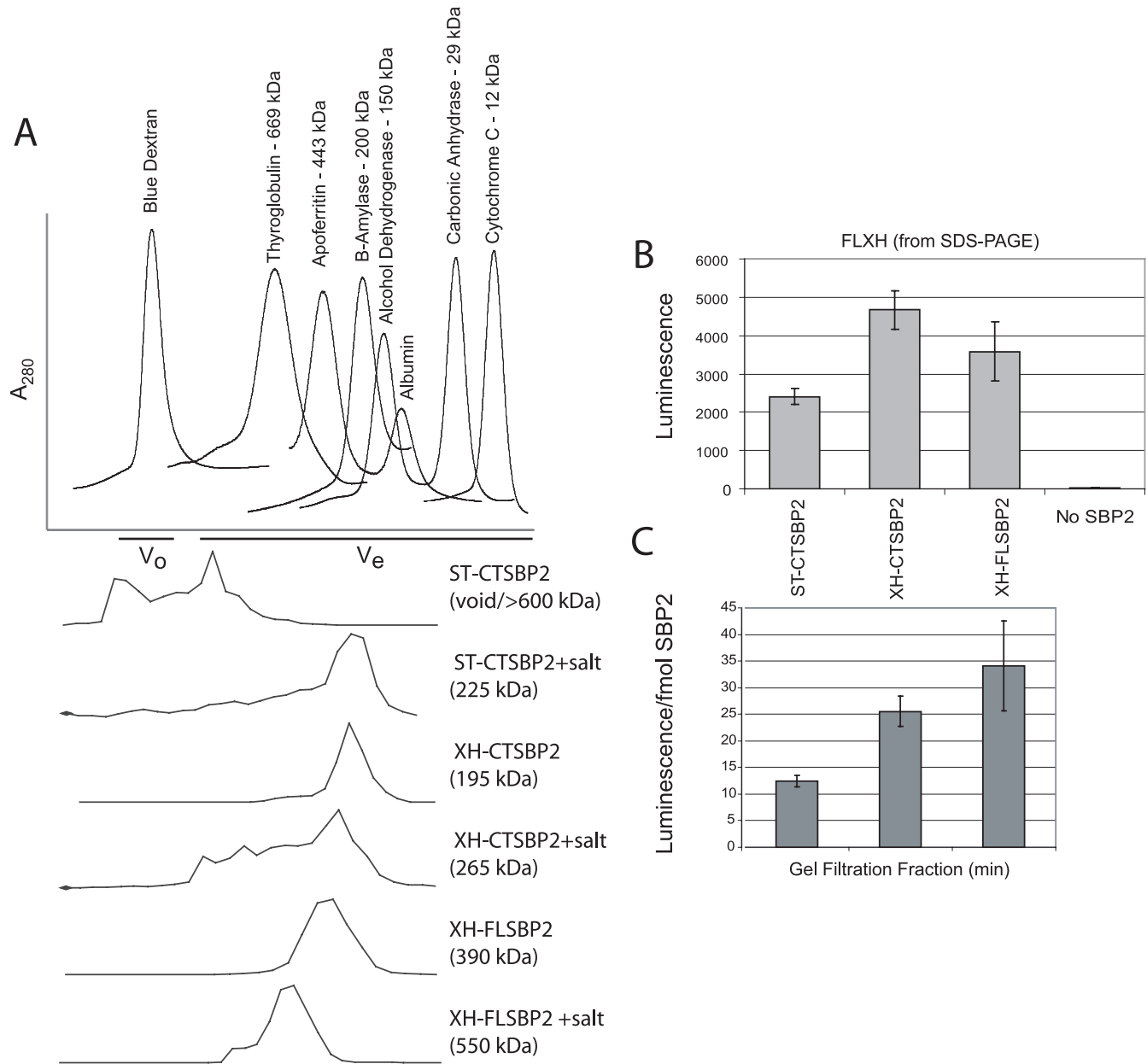
Figure 1. Molecular weight determination for SBP2. (**A**) A sample of 75 µg of C-terminal or full-length SBP2 as indicated was resolved by Sephadex 200 gel filtration chromatography. Fractions were analyzed by SDS–PAGE followed by Coomassie staining and densitometry. The density peaks were aligned with their corresponding position on overlaid chromatograms of the proteins used as standards (top). Calculated molecular weights for Strep-tagged CTSBP2 (ST-CTSBP2), Xpress/His-tagged C-terminal SBP2 (amino acids 399–846; XH-CTSBP2) and Xpress/His-tagged full-length SBP2 (XH-FLSBP2) in the presence (+salt) or absence of 1 M NaCl are shown on the right. (**B**) Samples of 10 ng of each type of SBP2 (as indicated) were added to a reticulocyte lysate assay containing luciferase mRNA with a Sec codon at position 258 and a wild-type GPX-4 SECIS element inserted in the 3′-untranslated region. The average luciferase activity (±SD) is shown for each version of SBP2. The data for the fourth column are from a reaction lacking any added SBP2. (**C**) The data in B re-plotted as luminescence units per fmol of SBP2.

the higher molecular weight complex identified in the low-salt conditions corresponds to untagged SBP2 interacting with *E.coli* ribosomes. Indeed, untagged SBP2 can be recovered in the ribosomal fraction during ultracentrifugation of *E.coli* extracts (data not shown), suggesting that the ribosomal element interacting with SBP2 is conserved from bacteria to mammals. The calculated molecular weight in high salt is very similar to that obtained for XH-CTSBP2 in low salt, suggesting that the XH tag may contribute to the apparent salt-dependent increase in size observed in Figure 1A. In addition,
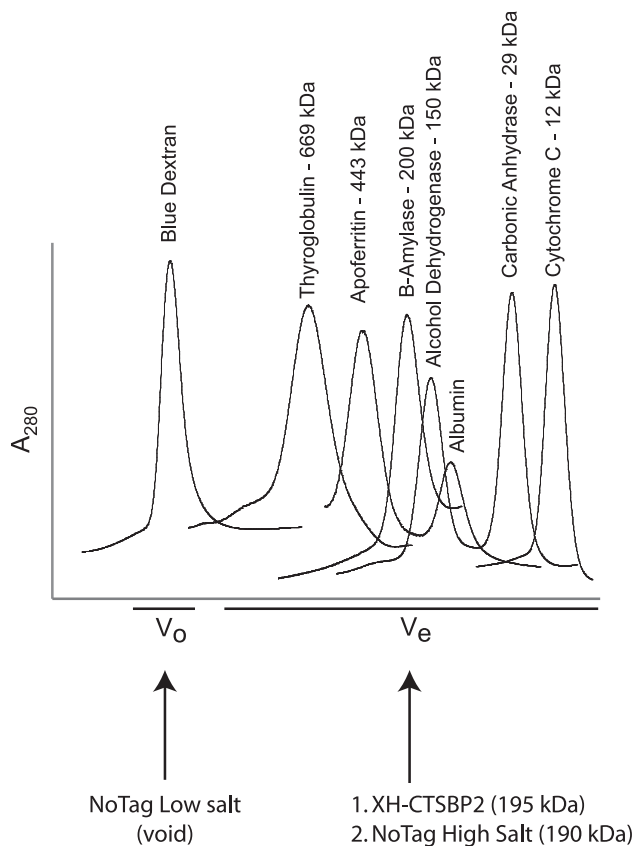
these results allow us to conclude that the discrepancy between predicted and observed molecular weight for SBP2 is intrinsic to its structure.

SBP2 in cell extracts sediments as a 5 MDa complex due to ribosome association

In order to study the SBP2 complex in mammalian cells, we determined the apparent molecular weight for SBP2 in McArdle 7777 cell extracts stably expressing full-length
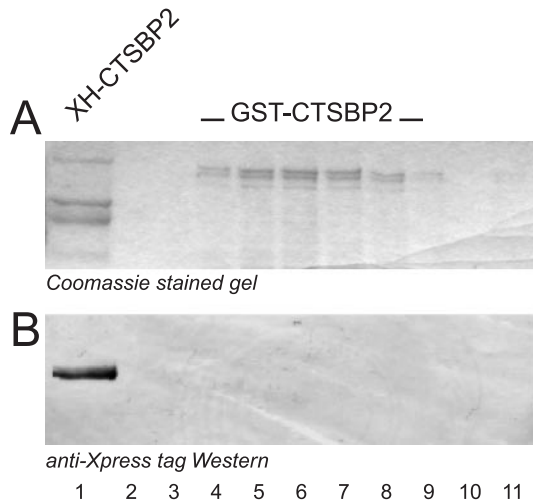
Figure 2. (**A** and **B**) XH-CTSBP2 fails to co-purify with GST-CTSBP2. Both XH-CTSBP2 and GST-CTSBP2 were co-expressed in *E.coli* and crude extracts were passed over a glutathione agarose column. Fractions were tested for GST-CTSBP2 content by SDS–PAGE and Coomassie staining. Each fraction was also tested for the presence of XH-CTSBP2 by western analysis using an anti-Xpress tag antibody. Lane 1 shows 20 ng of recombinant XH-tagged SBP2 purified on Nickel-agarose from the co-expressing strain.

SBP2 bearing N-terminal V5 and His tags (VH-FLSBP2). Initial experiments using Sephadex 200 gel filtration chromatography indicated that the native VH-FLSBP2 complex was in the void fraction and outside the resolving power of that column (data not shown). To resolve larger complexes, we fractionated the same extract on a Sephacryl S-500 column. Figure 4A shows that under low-salt conditions, VH-FLSBP2 elutes with a ∼5 MDa complex, the expected size for eukaryotic ribosomes (18). Under high ionic strength conditions, SBP2 is shifted to a much smaller size (∼500 kDa; Figure 4B), closely corresponding to the size of purified XH-FLSBP2 in high-salt conditions as shown in Figure 1A (550 kDa). To verify this correlation, we resolved purified XH-FLSBP2 under low-salt conditions and found that it eluted at ∼500 kDa as well (Figure 4D). These conditions are unable to resolve the difference between FLSBP2 run in high salt versus low salt as described above (data not shown). In order to demonstrate that the shift of SBP2 to the higher molecular weight fractions is due to ribosome binding, we incubated XH-FLSBP2 with purified, salt-washed rat ribosomes and fractionated the mixture by Sephacryl S-500 chromatography. Figure 4C shows that ribosomes alone are able to shift SBP2 to the same high molecular weight fraction found in crude cell lysates. These results indicate that SBP2 is quantitatively associated with the ribosomal fraction and that ribosomes can account for the entire difference between low- and high-salt conditions.
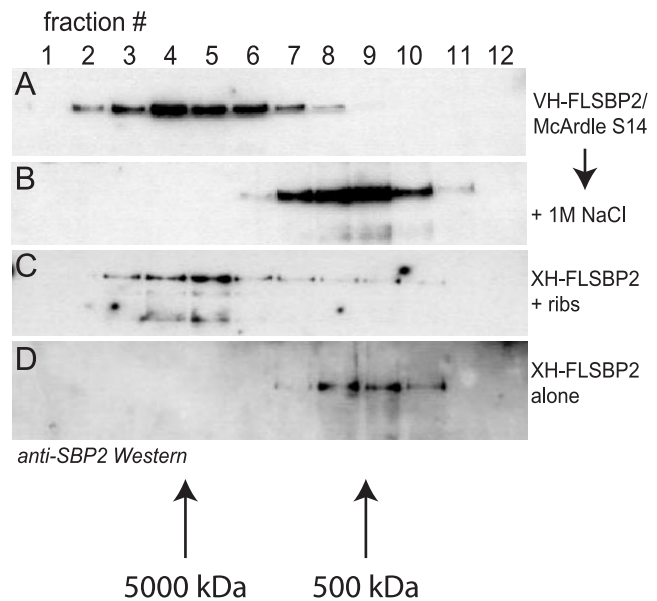

Figure 4. SBP2 is quantitatively associated with the ribosomal fraction. (**A**) A sample of 1.25 mg of cytoplasmic extracts (14 000 *g* supernatants [S14]) from McArdle 7777 cells stably expressing V5/His-tagged FLSBP2 (VH-FLSBP2) were resolved by Sephacryl S-500 gel filtration chromatography in either low salt (150 mM NaCl) or high salt (1 M NaCl) (**B**) or as indicated. Fractions were analyzed by western analysis using an anti-V5 antibody. (**C**) Purified XH-FLSBP2 (30 pmol) was chromatographed under the same conditions in the presence of 2 nmol purified salt-washed rat ribosomes. (**D**) A sample of 300 pmol of XH-FLSBP2 was chromatographed in the absence of added ribosomes. The fractions for (C) and (D) were analyzed by western analysis using an anti-SBP2 antibody. The calculated peak molecular weights are shown at the bottom.

Figure 3. Gel filtration of untagged CTSBP2. Samples of 5 mg of crude *E.coli* extracts containing untagged CTSBP2 were resolved by Sephadex 200 gel filtration chromatography in the presence and absence of 1 M NaCl. Fractions were analyzed by western analysis using affinity-purified anti-SBP2 antibody. The position of peak fractions relative to standards is shown by an arrow along with calculated molecular weight. The elution time for XH-CTSBP2 is shown for reference.

SBP2 cannot simultaneously bind to the ribosome and the GPX-4 SECIS element

We have previously reported that SBP2 is associated with ribosomes at the level of 28S rRNA interaction (8). Our original hypothesis that SBP2 was at least a dimer suggested a model where one subunit interacted with a kink-turn in 28S rRNA (there are potentially seven kink-turn motifs in mammalian 28S rRNA). Since we have shown that SBP2 is most likely monomeric, we wanted to determine whether SBP2 could simultaneously interact with the ribosome and a SECIS element. For this experiment, a 5-fold molar excess of either wild-type or mutant ^{32}P-labeled GPX-4 SECIS element was added to an SBP2 ribosome binding assay. We used a sucrose cushion assay to evaluate ribosome binding where a 2.5-fold molar excess of ribosomes relative to XH-CTSBP2 causes most of the SBP2 to pellet through the cushion. Figure 5A demonstrates that a 5-fold molar excess of wild-type GPX-4 SECIS element relative to XH-CTSBP2 is able to effectively compete SBP2 off of pre-formed SBP2/ribosome complexes albeit incompletely (compare lanes 6 and 7 with 79% of the SBP2 pelleting to lanes 8 and 9 with 49% pelleting). When a mutant SECIS element lacking the core AUGA motif required for SBP2 binding is used, no competition is observed (compare lanes 6 and 7 with 10 and 11 with 75% pelleting). When a mutant SECIS element lacking the conserved loop region not required for SBP2 binding is used, competition is once again evident as it reduced the amount of pelleted SBP2 to 40%. In order to determine if any of the SECIS element was found in the ribosomal fraction in an SBP2-dependent manner, RNA was extracted from both supernatant and pellet fractions and the RNAs resolved by denaturing polyacrylamide gel electrophoresis. Figure 5A (lower panel) clearly shows that the radiolabeled SECIS RNA is not associated with the pellet fractions therefore indicating that SBP2 cannot simultaneously associate with the ribosome and a SECIS element.

Since these experiments do not replicate Sec incorporation, but simply represent a simple *in vitro* competition assay, we chose to test whether similar results would be obtained during active translation of a full-length selenoprotein mRNA. To that end, a similar experiment was performed in rabbit reticulocyte lysate using varying amounts of full-length GPX-4 mRNA harboring either a wild-type or mutant SECIS element lacking the conserved AUGA motif. GPX-4 mRNAs were translated in reticulocyte lysate containing pre-translated FLSBP2. After 30 min, EDTA was added to release
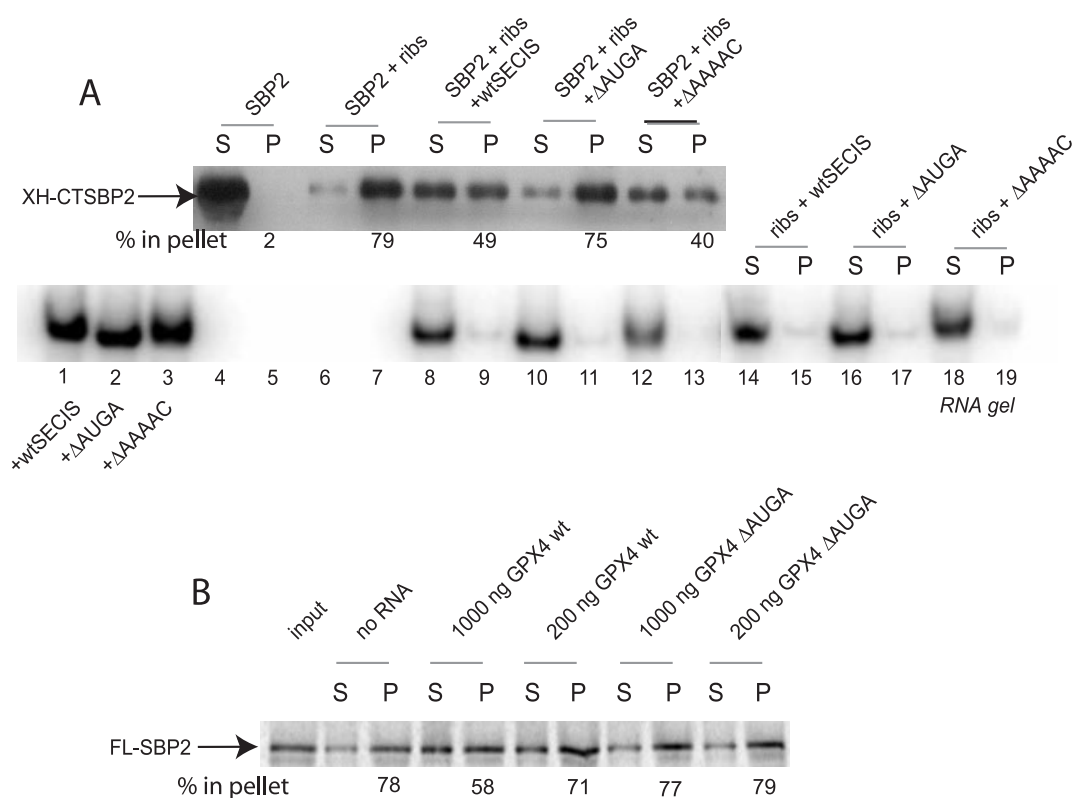
Figure 5. The SECIS element competes for ribosome binding to SBP2. (**A**) Reactions containing 6 pmol XH-CTSBP2, 15 pmol purified salt-washed rat ribosomes (+ribs) and 25 pmol ^{32}P-UTP-labeled wild-type (wt) or mutant SECIS element (ΔAUGA, ΔAAAAC) as indicated were layered onto 200 μl of 20% sucrose cushions followed by ultracentrifugation. Each supernatant (S) or pellet (P) (5%) was analyzed by SDS–PAGE and western analysis using an anti-Xpress tag antibody (top panel). The percent of XH-CTSBP2 in the pellet fractions is indicated below the panel as determined by densitometry. RNA was extracted from the remainder of the supernatant and pellet fractions and subjected to 5% denaturing PAGE (bottom panel). Lanes 1–3 correspond to the input SECIS RNAs, lanes 4–7 are derived from reactions lacking SECIS RNA, lanes 8–13 are derived from reactions containing all components, and lanes 14–19 correspond to reactions lacking SBP2. (**B**) Wild-type or mutant (ΔAUGA) full-length GPX-4 mRNA (200 or 1000 ng as indicated) was added to an *in vitro* translation reaction containing pre-translated, ^{35}S-labeled full-length SBP2 (FLSBP2). After 30 min of continued translation, EDTA was added to a final concentration of 5 mM in order to release mRNA from polysomes. The reactions were then layered onto sucrose cushions and analyzed for ribosome binding as described in (A). Radiolabeled SBP2 was detected by PhosphorImager analysis.
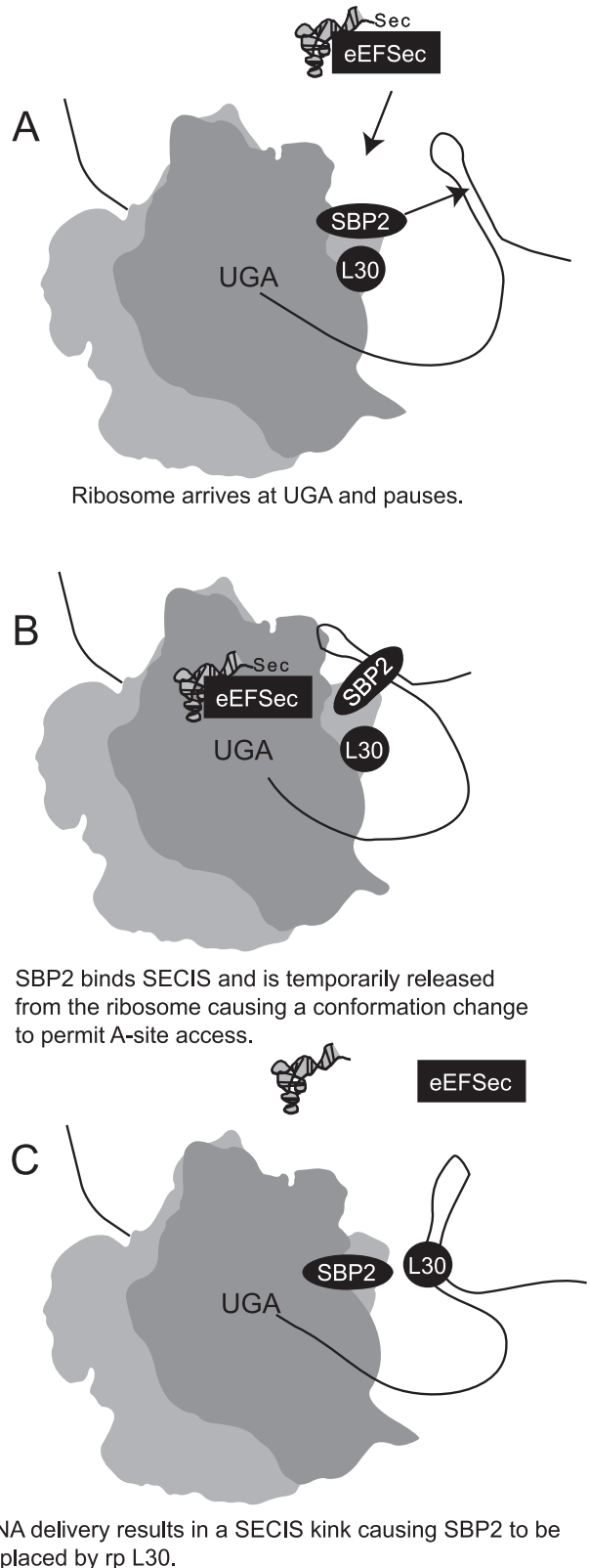
mRNA from ribosomes. If SBP2 were able to simultaneously bind the SECIS element and the ribosome during translation, all components would be found in the ribosomal pellet, even in the presence of EDTA, which does not affect SBP2/SECIS or SBP2/ribosome interactions (8,19). If however, SBP2 shifted to SECIS element binding during translation, then at the time of EDTA addition, all of the SBP2 actively engaged in Sec incorporation would be shifted to the supernatant. Figure 5B shows that full-length GPX4 mRNA is also able to compete for SBP2 binding under conditions where active translation and Sec incorporation is occurring, as evidenced by the production of full-length GPX4 protein in reactions containing wild-type GPX4 mRNA (data not shown). These data further demonstrate that SBP2 is unable to simultaneously bind the ribosome and the SECIS element. The same results were obtained when the C-terminal fragment of SBP2 was used instead of full-length protein (data not shown). Thus, using purified components *in vitro* as well as in an *in vitro* translation system, these experiments indicate that SBP2 is likely to shift off of ribosomes and onto the SECIS element during Sec incorporation.

DISCUSSION

The results presented herein allow us to conclude two important points regarding Sec incorporation: SBP2 does not self-associate and SBP2 cannot simultaneously interact with a SECIS element and the ribosome. Thus, we propose a distinct model for Sec incorporation based on these and other recent findings including a role for non-ribosome bound rpL30 in SECIS element binding (Figure 6). In order for the model to fit the idea that SBP2 is ribosome bound but cannot simultaneously bind the SECIS element, it is necessary to invoke a scenario where SBP2 interacts with a SECIS element co-translationally thus allowing eEFSec/Sec-tRNA$^{[Ser]Sec}$ access to the ribosomal A-site. A possible role for rpL30, therefore might be to allow SBP2's reassociation with the ribosome by competing for SECIS element binding under those conditions.

In contradiction to previous hypotheses, SBP2 does not act as a dimer or other homomultimer. The previous assumptions were based on the Strep-tagged version of SBP2 which we demonstrate here forms an artificially large Strep-tag-dependent complex. Since SBP2 dimerization was a pre-requisite of the model where SBP2 could simultaneously interact with both a SECIS element and the ribosome, we sought to directly test that hypothesis. By demonstrating that a SECIS element, as well as a full-length selenoprotein mRNA, can effectively compete for ribosome binding, it is clear that the previous model was incorrect and that the SBP2/SECIS element interaction excludes ribosome binding, at least *in vitro*. Further experiments will be required to test the relative affinities and the sequence specificity of rRNA binding to gain insight into the interplay between rRNA and SECIS element binding.

The fact that a SECIS element excludes ribosome binding provides further evidence that SBP2 is likely to be interacting with the ribosome at one of the kink-turn elements within 28S rRNA. However, this hypothesis is in conflict with the fact that a mutation in a conserved residue within the core L7Ae

Ribosome arrives at UGA and pauses.

SBP2 binds SECIS and is temporarily released from the ribosome causing a conformation change to permit A-site access.

tRNA delivery results in a SECIS kink causing SBP2 to be displaced by rp L30.

Figure 6. A revised model for Sec incorporation. (**A**) The SECIS element is recognized by SBP2 when the ribosome pauses at the Sec codon. (**B**) Instead of termination, Sec is incorporated as SBP2 binds to the SECIS element and allows eEFSec/Sec-tRNA$^{[Ser]Sec}$ access to the ribosomal A-site. (**C**) After tRNA dissociation, rpL30 binds to the altered SECIS element conformation allowing SBP2 to re-associate with the ribosome.

RNA binding domain in SBP2 (G699R), which results in eliminating SECIS element binding, retained its ability to bind ribosomes (8). In addition, the same report demonstrated that the SBP2 functional domain (amino acids 399–517) is required for full ribosome binding activity. Taken together, this suggests that SBP2 may possess multiple ribosome contact sites and may remain weakly associated with the ribosome during Sec incorporation, but not when challenged with a molar excess of SECIS element or full-length selenoprotein mRNA as described here.

Our initial observation of the SBP2 ribosome binding activity indicated that all of the transfected SBP2 was bound to ribosomes (8). Those experiments were performed using transient transfection in McArdle 7777 cells where transfection efficiency is generally low (∼20%). Thus, it is possible that the limited amount of SBP2 per cell allowed unbound SBP2 to associate with ribosomes during extraction. Using gel filtration chromatography, we have demonstrated similar results, but using cells stably transfected with SBP2. These results support the idea that SBP2 is stably bound to ribosomes suggesting that SECIS element interactions only occur on actively translating selenoprotein mRNAs. This result appears to be in conflict with a previous report showing that SECIS-containing mRNAs co-immunoprecipitated with SBP2. However, all of the mRNA detected in that experiment could have derived from the actively translating pool—a possibility that was not investigated at that time (6). It is intriguing to note that SBP2 apparently shows ribosome binding activity to *E.coli* ribosomes (Figure 3). This combined with the fact that SBP2 also binds to yeast ribosomes (an organism lacking Sec; Paul R. Copeland, unpublished results) suggests that the SBP2 binding site is a universally conserved ribosomal feature, perhaps not surprising for a binding site targeted by a factor that regulates processes as generally conserved as translation elongation and termination.

ACKNOWLEDGEMENTS

Conflict of interest statement. None declared.

REFERENCES

1. Driscoll,D.M. and Copeland,P.R. (2003) Mechanism and regulation of selenoprotein synthesis. *Annu. Rev. Nutr.*, **23**, 17–40.
2. Hatfield,D.L. and Gladyshev,V.N. (2002) How selenium has altered our understanding of the genetic code. *Mol. Cell. Biol.*, **22**, 3565–3576.
3. Howard,M.T., Aggarwal,G., Anderson,C.B., Khatri,S., Flanigan,K.M. and Atkins,J.F. (2005) Recoding elements located adjacent to a subset of eukaryal selenocysteine-specifying UGA codons. *EMBO J*, **24**, 1596–1607.
4. Fagegaltier,D., Hubert,N., Yamada,K., Mizutani,T., Carbon,P. and Krol,A. (2000) Characterization of mSelB, a novel mammalian elongation factor for selenoprotein translation. *EMBO J.*, **19**, 4796–4805.
5. Tujebajeva,R.M., Copeland,P.R., Xu,X.-M., Carlson,B.A., Harney,J.W., Driscoll,D.M., Hatfield,D.L. and Berry,M.J. (2000) Decoding apparatus for eukaryotic selenocysteine insertion. *EMBO Rep.*, **1**, 1–6.
6. Copeland,P.R., Fletcher,J.E., Carlson,B.A., Hatfield,D.L. and Driscoll,D.M. (2000) A novel RNA binding protein, SBP2, is required for the translation of mammalian selenoprotein mRNAs. *EMBO J*, **19**, 306–314.
7. Chavatte,L., Brown,B.A. and Driscoll,D.M. (2005) Ribosomal protein L30 is a component of the UGA-selenocysteine recoding machinery in eukaryotes. *Nat Struct. Mol. Biol.*, **12**, 408–416.
8. Copeland,P.R., Stepanik,V.A. and Driscoll,D.M. (2001) Insight into mammalian selenocysteine insertion: domain structure and ribosome binding properties of sec insertion sequence binding protein 2. *Mol. Cell. Biol.*, **21**, 1491–1498.
9. Mehta,A., Rebsch,C.M., Kinzy,S.A., Fletcher,J.E. and Copeland,P.R. (2004) Efficiency of mammalian selenocysteine incorporation. *J. Biol. Chem.*, 37852–37859.
10. Klein,D.J., Schmeing,T.M., Moore,P.B. and Steitz,T.A. (2001) The kink-turn: a new RNA secondary structure motif. *EMBO J.*, **20**, 4214–4221.
11. Koonin,E.V., Bork,P. and Sander,C. (1994) A novel RNA-binding motif in omnipotent suppressors of translation termination, ribosomal proteins and a ribosome modification enzyme? *Nucleic Acids Res.*, **22**, 2166–2167.
12. Vilardell,J., Yu,S.J. and Warner,J.R. (2000) Multiple functions of an evolutionarily conserved RNA binding domain. *Mol. Cell*, **5**, 761–766.
13. Fletcher,J.E., Copeland,P.R., Driscoll,D.M. and Krol,A. (2001) The selenocysteine incorporation machinery: interactions between the SECIS RNA and the SECIS-binding protein SBP2. *RNA*, **7**, 1442–1453.
14. Allmang,C., Carbon,P. and Krol,A. (2002) The SBP2 and 15.5 kD/Snu13p proteins share the same RNA binding domain: identification of SBP2 amino acids important to SECIS RNA binding. *RNA*, **8**, 1308–1318.
15. Copeland,P.R. (2003) Regulation of gene expression by stop codon recoding: selenocysteine. *Gene*, **312**, 17–25.
16. Lesoon,A., Mehta,A., Singh,R., Chisolm,G.M. and Driscoll,D.M. (1997) An RNA-binding protein recognizes a mammalian selenocysteine insertion sequence element required for cotranslational incorporation of selenocysteine. *Mol. Cell. Biol.*, **17**, 1977–1985.
17. Algire,M.A., Maag,D., Savio,P., Acker,M.G., Tarun,S.Z.,Jr, Sachs,A.B., Asano,K., Nielsen,K.H., Olsen,D.S., Phan,L. *et al.* (2002) Development and characterization of a reconstituted yeast translation initiation system. *RNA*, **8**, 382–397.
18. Tashiro,Y. and Siekevitz,P. (1965) Ultracentrifugal studies on the dissociation of hepatic ribosomes. *J. Mol. Biol.*, **11**, 149–165.
19. Copeland,P.R. and Driscoll,D.M. (1999) Purification, redox sensitivity, and RNA binding properties of SECIS-binding protein 2, a protein involved in selenoprotein biosynthesis. *J. Biol. Chem.*, **274**, 25447–25454.